Methodology document for the WHO e-atlas of disaster risk.

Volume 1. Exposure to natural hazards

Version 2.0

Landslide hazard modelling

Dr Zine El Abidine El Morjani

Taroudant poly-disciplinary faculty
of the Ibn Zohr University of Agadir, Morocco

Last Update: January 2011

Cataloguing-in-Publication Data

Methodology document for the WHO e-atlas of disaster risk. Volume 1. Exposure to natural hazards Version 2.0: Landslide hazard modelling

1. Disasters – Landslide. 2. Geographic Information Systems. 3. Risk Management.

ISBN: 978-9954-0-5394-2

© Ibn Zohr University, 2011

All rights reserved. Publications of the Ibn Zohr University can be obtained from Ibn Zohr University, BP 32/S Agadir, Morocco (tel.: +212 528 22 71 25; fax: +212 528 22 72 60; e-mail: Eddaoudi@univ-ibnzohr.ac.ma). Requests for permission to reproduce or translate Ibn Zohr publications – whether for sale or for noncommercial distribution – should be addressed to Ibn Zohr University, at the above contact details.

The designations employed and the presentation of the material in this publication do not imply the expression of any opinion whatsoever on the part of the Ibn Zohr University concerning the legal status of any country, territory, city of area or of its authorities, or concerning the delimitation of its frontiers or boundaries. Dotted lines on maps represent approximate border lines for which there may not yet be full agreement.

All reasonable precautions have been taken by the Ibn Zohr University to verify the information contained in this publication. However, the published material is being distributed without warranty of any kind, either expressed or implied. The responsibility for the interpretation and use of the material lies with the reader. In no event shall the Ibn Zohr University be liable for damages arising from its use.

Acknowledgements

The development of the methodology for the preparation of the landslide hazard distribution map is the product of contributions by several institutions and individuals. The funding to conduct the research leading to the development of the protocol has been provided by the World Health organization (WHO). The elaboration of the models was carried out by Zine El Abidine El Morjani, Taroudant poly-disciplinary faculty of the Ibn Zohr University of Agadir, Morocco and Steeve Ebener, WHO Mediterranean Centre for Health Risk Reduction, Tunisia. The data collection and analysis, implementation of the models, and documentation of the methodology were carried out by Zine El Abidine El Morjani.

Contents

Preface

Being able to conduct geographically based risk assessment at the sub national level requires being in a position to spatially distribute all the elements reported in following conceptual formula[1]:

$$\text{Risk} \propto \frac{\text{Hazard x Vulnerability}}{\text{Capacity}}$$

This process being very much driven by the type of hazard faced by the population and/or the key infrastructures in a given country the World Health Organization has been working, since 2006 on the development and improvement of an electronic atlas which could stimulate ministries of health and other health stakeholders to improve their disaster management capacity as well as serve as the entry point for conducting sub national geographically based risk assessments.

The WHO e-atlas of disaster risk models the distribution of natural hazards and population's exposure and provides baseline data and maps needed to advocate for resources to improve disaster preparedness; aid emergency response measures; and assist in identifying, planning and prioritizing areas for mitigation activities.

The first version of the e-atlas published in 2008 covered the WHO Eastern Mediterranean Region (22 countries) and five natural hazards (flood, seismic [earthquake], landslide, heat and wind speed) and was distributed to more than 500 users.

Encouraged by this success, working in close collaboration with the WHO Regions and taking advantage of the establishment of the Vulnerability and Risk Analysis and Mapping programme (VRAM), it was decided to publish a second version of the e-atlas that would, this time, also the 46 countries forming the WHO African Region as well as 32 countries of the WHO European Region (due to limited resources, this version of the e-atlas focuses on Central Europe only).

Building on the successful collaboration established between the Taroudant polydisciplinary faculty of Ibn Zohr University, Agadir, Morocco and the VRAM, most of the models used in the first version of the e-atlas have been improved and heat replaced by heat wave, a current preoccupation of many ministries of health.

In order to allow for any other region or country to also apply the models on their own it has been decided to document not only the research behind the models but also provide users with a protocol that would allow them to generate the final hazard distributions maps. The present series of methodology document is the result of this documentation.

---

[1] Modified from: Office of the United Nations Disaster Relief Co-ordinator (UNDRO). *Mitigating natural disasters. phenomena, effects and options. A manual for policy makers and planners*. New York, United Nations, 1991.

It is important to underline that the hazard distribution maps resulting from the application of these models are nevertheless only the first step of a process allowing countries to assess their risk at the sub national level.

Analysing vulnerability and capacity require a process which is difficult to be applied at the level of a region for the following reasons:

- availability of desegregated data
- incompatibility of indicators from one country to an other
- important differences in terms of health context between one country and another.

WHO has therefore been looking at having the vulnerability, capacity and therefore indirectly risk analysis, conducted on a country by country basis.

In this context, the VRAM is supporting Member States and partners to strengthen their capacity in order to conduct such analysis and have it presented in a manner such as the figure below.

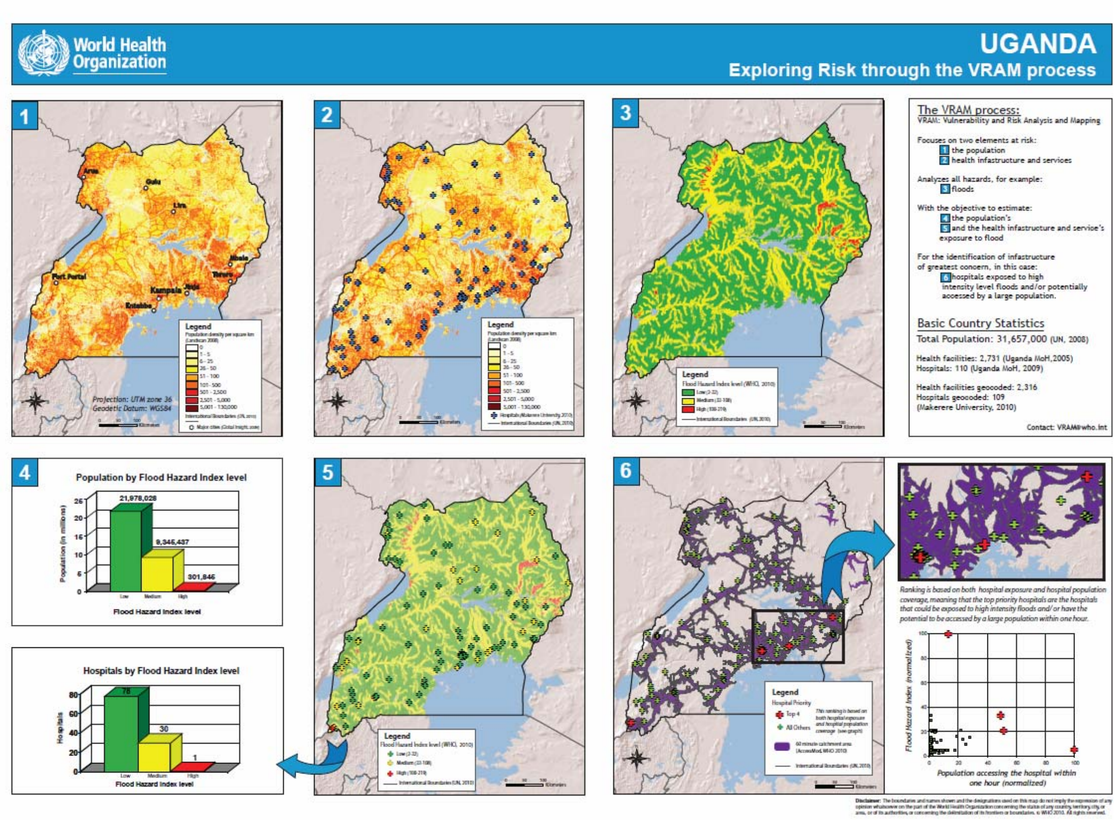

The VRAM process:
VRAM: Vulnerability and Risk Analysis and Mapping

Focuses on two elements at risk:
1 the population
2 health infastructure and services

Analyzes all hazards, for example:
3 floods

With the objective to estimate:
4 the population's
5 and the health infastructure and service's exposure to flood

For the identification of infrastructure of greatest concern, in this case:
6 hospitals exposed to high intensity level floods and/or potentially accessed by a large population.

Basic Country Statistics
Total Population: 31,657,000 (UN, 2008)

Health facilities: 2,731 (Uganda MoH,2005)
Hospitals: 110 (Uganda MoH, 2009)

Health facilities geocoded: 2,316
Hospitals geocoded: 109
(Makerere University, 2010)

Contact: VRAM@who.int

Ranking is based on both hospital exposure and hospital population coverage, meaning that the top priority hospitals are the hospitals that could be exposed to high intensity floods and/or have the potential to be accessed by a large population within one hour.

The result of such analysis is then to be integrated in the country Disaster Risk Reduction (DRR) and Health Emergency Preparedness and Response Programmes (HEPRP) and serve, among other things, to build safer hospital, improve mass casualties' management and help specialized units within health Organizations (including MoH) for public health planning.

At the same time, the baseline data, information and maps collected or produced through the process can be used by health authorities and partners to take informed decisions in times of crises.

1. Introduction

This document describes the methodology and protocol developed by the Taroudant polydisciplinary faculty of Ibn Zohr University in close collaboration with the VRAM and then used to generate and document maps presenting the spatial distribution of landslide hazard for the *WHO e-atlas of disaster risk, volume 1: exposure to natural hazards, Version 2.0.*

The methodology used to distribute landslide hazard is based on a derivative multi-criteria analysis (MCA) that classifies areas according to the likelihood of a landslide's occurrence on their surface, which in some cases is described as landslide susceptibility.

The methods and process presented in this document could be applied to other geographic areas provided that the analyses use geospatial data of similar or better quality and resolution.

2. Methodology

Many methods and techniques have been proposed in the literature for the evaluation and zonation of landslide hazards. Landslide hazard maps can be produced either by using qualitative (direct) or quantitative (indirect) mapping techniques [Hansen, 1984; Hansen and Frank, 1991].

Qualitative techniques consist of a geomorphological mapping exercise in which a geomorphologist identifies past landsides and, with the insight of previous knowledge and experience, develops postulations as to the likelihood of future slope failures. While this traditional technique yields effective hazard zonation maps, it is time-consuming, expensive and extremely labour-intensive. Due to these drawbacks and the refinement of effective indirect mapping techniques, it is not widely applied.

Quantitative techniques adopt either a deterministic or a statistical model to develop landslide hazard zone boundaries. The deterministic approach is based on prior knowledge of the physical factors that are at the origin of landslides. Instability factors are mapped, ranked and weighted based on their assumed or expected importance in causing mass-wasting [Gupta and Joshi, 1990; Pachauri and Pant, 1992; Maharaj, 1993; Anbalagan and Singh, 1996; Gökçeoğlu and Aksoy, 1996; Turrini and Visintainer, 1998; Pachauri et al., 1998; Barredo et al., 2000; Wachal and Hudak, 2000; Donati and Turrini, 2002; Esmali and Ahmadi, 2003; Ayenew and Barbieri, 2005]. The combination of the weighted instability factor layers yields a single surface that quantifies the likelihood of a mass-wasting event to occur in a specific geospatial location.

A statistical or probabilistic model uses the observed relationships between each instability factor and past landslides to establish a factor's role in the mass-wasting process and calculates the likelihood of a future mass-wasting event at a specific location [Gupta and Joshi, 1990; Clerici et al., 2002; Dai and Lee, 2002; Donati and Turrini, 2002; Ercanoğlu et al., 2004; Suzen and Doyuran, 2004; Ayalew and Yamagishi, 2004]. A probabilistic model can use any number of statistical techniques including bivariate or multivariate statistical analysis regression.

Each technique and model has a unique set of advantages and disadvantages. For this reason, there is no consensus among researchers on the best or most appropriate model to be used in order to identify and map mass-wasting–prone areas [Brabb, 1984; Carrara, 1989].

Nevertheless, the absence of any comprehensive past landslide inventory for the countries in the WHO Regions (AFRO, EMRO, part of the EURO) obliged us to use a deterministic model in order to determine landslide susceptibility over this area as an approximation of landslide hazard.

There are two additional advantages in using a deterministic model. First, this approach is compatible with computerized geospatial methods and geocomputational techniques. Second, results yielded from the model can be readily assessed and recreated.

The method is implemented as following (Figure 1):

- identification of the causal factors
- reclassification of the slope map
- except for slope, normalisation of the causal factors to obtain a continuous scale
- prioritization (weighting) of the causal factors
- creation of the intermediate susceptibility landslide susceptibility distribution maps.
- combination of the landslide susceptibility distribution map with the slope distribution to create the final landslide hazard distribution map.

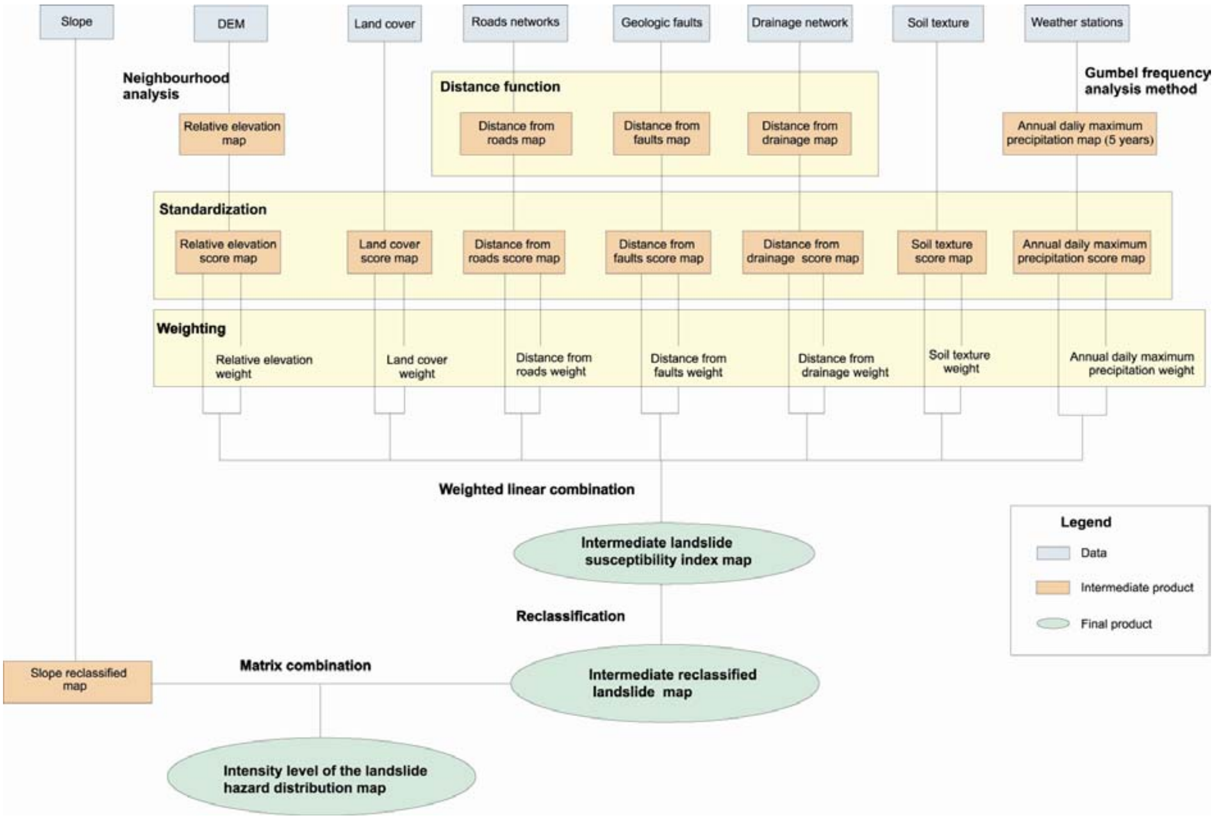

Figure 1. Methodology for the generation of the spatial distribution of the intensity levels of landslide hazards

2.1 Identification of the causal factors

The methodology described in this document uses a composite landslide hazard index based on eight causal factors. These factors, which are listed here, have been selected based on different case studies of relevance to the region covered in this version of the e-atlas.

- *Slope*. The likelihood of a landslide increases as slope increases [Roth, 1983; Barisone and Bottino, 1990; Koukis and Ziourkas, 1991; Anbalagan, 1992; Pachauri and Pant, 1992; Maharaj, 1993; Jager and Wieczorek, 1994; Anbalagan and Singh, 1996; Talib, 1997; Atkinson and Massari, 1998; Baum et al., 1998; Guzzetti et al., 1999; Zezere et al., 1999; Sinha et al., 1999; Guzzetti et al., 2000; Jakob, 2000; Nagarajan et al., 2000; Ramakrishnan, 2002; Esmali and Ahmadi 2003; Kelarestaghi, 2003; Tangestani, 2003; Van Westen, 2003; Duman et al., 2005; Gomes et al., 2005, Komac and Ribičič, 2006].

- *Relative elevation*. This is the greatest difference in elevation which exists between a cell and the lowest adjacent cell. The likelihood of a landslide increases as the relative elevation of a location increases [Pachauri and Pant, 1992; Talib, 1997; Sinha et al., 1999; Ercanoğlu and Gökçeoğlu, 2002; Esmali and Ahmadi 2003; Tangestani, 2003; Kelarestaghi, 2003].

- *Annual daily maximum precipitation*. Precipitation is an important parameter that affects slope stability in two ways. First, precipitation can affect rock formations at considerable depths (up to 20 metres depending upon local geology) and increase the likelihood of landslides. In areas with high precipitation inputs, water can infiltrate tens of metres below the surface and promote rock weathering, which increases the likelihood of deep-seated landslides; second, precipitation increases the amount of water in surface soils which can increase the likelihood of mass-wasting events. Precipitation increases the saturation level of surface soils, which increases pore water pressure in the voids between soil particles. This increase in pore water pressure decreases the friction and cohesion between soil particles and can lead to shallow-seated landslides and debris flows. Several researchers [Esmali and Ahmadi, 2003; Kelarestaghi, 2003] consider precipitation to be a hugely critical factor in causing slope instability and landslides, second only to the force of gravity as exhibited in the slope and relative elevation of a location. In this study, the annual daily maximum precipitation has been calculated with a return period of five years calculated using the frequency analysis method called the Gumbel method. For specific information regarding the computing of this parameter, please see the *WHO/EMRO e-atlas of disaster risk methodology and implementation process for modelling the spatial distribution of landslide hazard* document that can be found on the e-atlas DVD.

- *Landcover*. Vegetation plays a critical role in slope stabilization through several processes. Root systems bind soil together and decrease soil water saturation; foliage intercepts precipitation and decreases its erosive effect on the soil surface; areas with little or no vegetative land cover and areas degraded by inappropriate logging, pastoral, agricultural or construction practices are predisposed to landslides and mass-wasting events [Swanson and Dyrness, 1975; Varnes, 1978; Sidle, Pearce, and O'Loughlin, 1985; Talib, 1997; Sinha et al., 1999; Ramakrishnan, 2002; Esmali and Ahmadi, 2003; Tangestani, 2003; Kelarestaghi, 2003; Komac and Ribičič, 2006].

- *Distance from roads*. The construction of roads that cross slopes can destabilize an area in two ways: first, the cut into the slope can increase the slope of an area, making it more prone to landslides; second, cutting a road at the foot of a slope removes lateral support from the slope and increases the likelihood of landslides [Varnes, 1984; Sidle, Pearce, and O'Loughlin, 1985; Talib, 1997; Sinha et al., 1999; Sarkar, 2002; Kelarestaghi, 2003; Tangestani, 2003; Esmali and Ahmadi 2003].

- *Distance from geological faults*. Local shocks and vibrations caused by seismic activity along geological faults can trigger landslides and other mass-wasting events. The likelihood of seismic shocks or earthquakes triggering a mass-wasting event increases as the distance between the fault and the slope decreases [Sinha et al., 1999; Sarkar, 2002; Esmali and Ahmadi, 2003; Tangestani, 2003, Kelarestaghi, 2003; Komac and Ribičič, 2006).

- *Distance from the drainage network*. Increasing the proximity of a slope to hydrological features such as streams, rivers or oceans can decrease slope stability in several ways. Streams and rivers may adversely affect slope stability by eroding the foot of a slope; this erosion, or undercutting, decreases the slope's lateral stability and increases the likelihood of failure; streams can saturate a slope and increase the soil's pore water pressure, leading to a decrease in the cohesion between soil particles and an overall destabilization of the slope; marine wave action coupled with beach erosion can steepen seaside slopes making them more susceptible to landslides during periods of high precipitation or cause catastrophic failure along geological joints, bedding, and exfoliation surfaces [Gökçeoğlu and Aksoy, 1996; Talib, 1997; Sinha et al., 1999; Sarkar, 2002; Tangestani, 2003; Esmali and Ahmadi 2003].

- *Soil texture*. This determines the internal cohesion and friction of a soil. Cohesion and friction determine the shear strength of a material. Cohesion is the tendency of soil particles to interlock and rest at an angle. Clayey soils and rocks are cohesive, sand is cohesionless. Cohesive forces operate independently of external loading (additional weight placed on the soil surface in the form of buildings, roads, vegetation, etc.). Friction is the tendency of soil particles to resist sliding across each other. Friction forces are dependent upon the load placed on the soil surface—the greater the load, the greater the likelihood that the forces of friction will be overcome. This results in the movement of soil particles within the soil layer and potentially to slope failure. [Ramakrishnan, 2002; Tangestani, 2003, Esmali and Ahmadi 2003; Duman et al., 2005; Komac and Ribičič, 2006].

- *Lithology*. Many sources identify lithology as a very important factor that can predispose an area to land slides and mass-wasting events [Glassey et al., 1997; Sinha and Mehta, 1999; Esmali and Ahmadi, 2003; Martinez, 2003; Van Westen, 2003; Duman et al., 2005]. However, lithology data for the region covered by this version of the e-atlas are not available. As a result, this factor is not included in the analysis.

2.2 Reclassification of the slope

Based on the relations studies between landslide distribution and slope steepness (Bender, 2001and Gomes et al., 2005), slopes (in percent) have been subdivided into 4 classes (table 1).

Table 1. Table used for the reclassification of the slope layer into ordinal values

Slope (%)	Ordinal value
0–12	1
12–25	2
25–50	3
≥50	4

2.3 Standardization of the other causal factors (except the slope) distribution according to a continuous scale

To integrate both the continuous and discrete forms of the causal factors (except the slope) into the multi-criteria analysis it is necessary to reclassify each of the layers concerned according to a comparable scale of ordinal classes, in our case going from 0 to 4; 0 corresponding to the classes where a landslide was the least likely to occur, and 4 to those where the likelihood was the highest.

The following sections describe how the reclassification took place depending on the type of data.

2.3.1 Reclassification of the continuous data layers

The majority of the causal factors used in the present methodology are continuous, meaning they are quantitative in nature, not restricted to taking on certain specified values, and the difference between any two values can be arbitrarily small. However, the units of measurement for the data vary from factor to factor. The data capture length (distance from hydrologic features, roads and faults, as well as relative elevation) and volumetric (annual daily maximum precipitation) measurements.

As there is no consensus among researchers regarding the precise nature of the relationships that exist between the proximity to road, rivers and faults features and landslide susceptibility, linear scaling has used to reclassify the distribution of these values according to a nominal scale. This is done using the following equation, which is a simple linear scaling equation where the raw value for any given pixel is denoted as *R* [Voogd, 1983; Eastman, 2003]:

$$x_i = \frac{(R_i - R_{\min})}{(R_{\max} - R_{\min})} \times \text{standardized range} \qquad \text{Equation 1}$$

with: x_i = ordinal value
R_i = raw data value.

This equation employs the minimum and maximum values ($R_{\min}$ and $R_{\max}$) present in the continuous layer as scaling points. The standardized range is the range of the values of the ordinal classes (4 in our case).

This equation is also used to positively correlate all causal factor data to landslide likelihood. In cases where there is an initial positive correlation (landslide likelihood increases as the value of the causal factor increases) $R_{\min}$ will be equal to the lowest raw value in the dataset and $R_{\max}$ will be equal to the highest raw value in the dataset. The causal factors with an initial positive correlation to landslide likelihood are relative elevation and annual daily maximum precipitation.

For example, Figure 2 presents an initial positive correlation between a causal factor and landslide susceptibility.

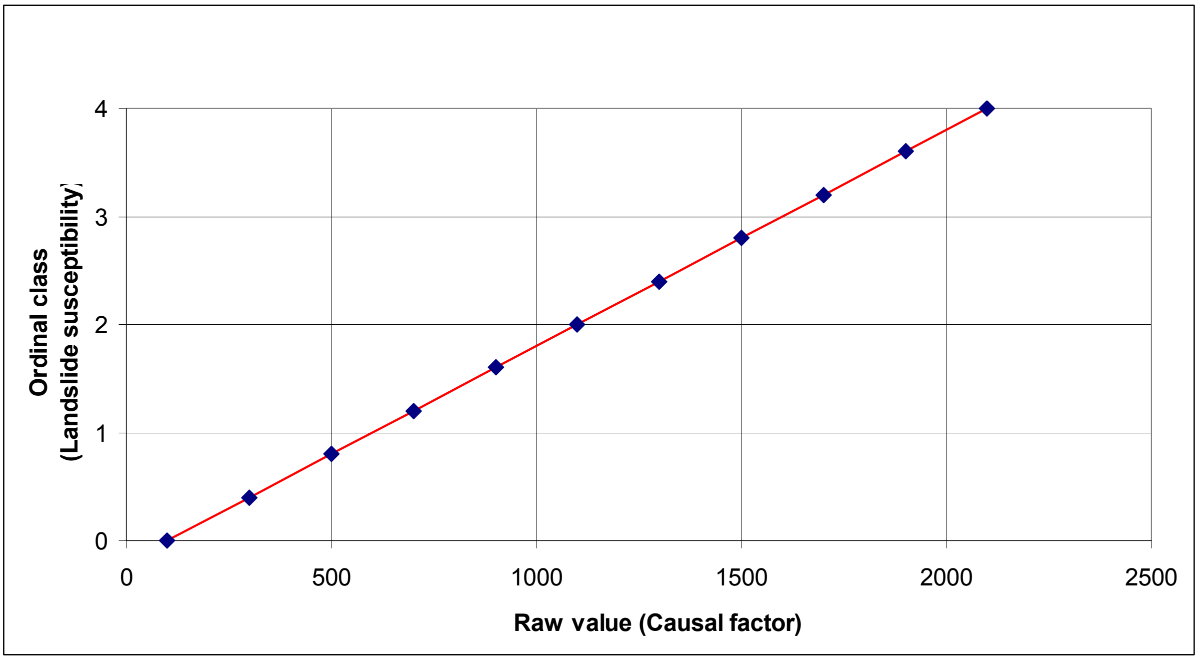

Figure 2. Example of positive correlation between raw values and an ordinal classification scheme

Conversely, when the correlation between the causal factor and the likelihood for a landslide to occur is negative (likelihood decreases as the value of the causal factor increases) $R_{\min}$ will be equal to the highest raw value in the dataset and $R_{\max}$ will be equal to the lowest raw value in the dataset. The causal factors with an initial negative correlation to landslide susceptibility are the distance from the hydrographic network, the roads and the faults.

As an example, Figure 3 presents an initial negative correlation between a causal factor and landslide susceptibility.

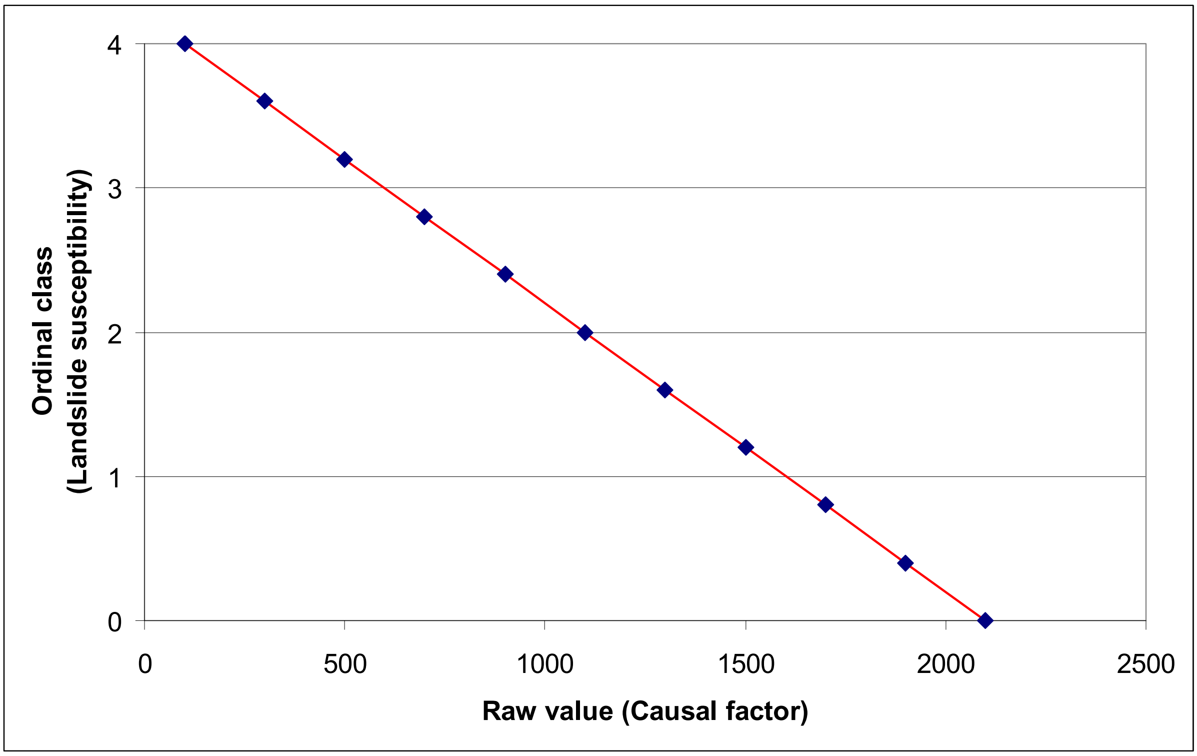

Figure 3. Example of negative correlation between raw values and an ordinal classification scheme

In view of the above, continuous data layers presenting a positive correlation with landslide susceptibility have been treated separately than those presenting a negative correlation.

2.3.1.1 Reclassification of causal factors presenting a negative correlation

As mentioned previously, the distance from hydrological features, roads and geological faults are the causal factors that present a negative correlation with landslide susceptibility (landslide susceptibility decreases as distance from a feature increases).

However there is no consensus among researchers regarding the precise nature of the relationships that exist between the proximity of these features and landslide susceptibility. As a result, different researchers delineate landslide susceptibility differently with similar distances from roads, drainage networks and geological faults [Anbalagan, 1992; Pachauri and Pant, 1992; Maharaj, 1993; Gökceoğlu and Aksoy, 1996; Luzi and Pergalani, 1999; Donati and Turrini, 2002; Esmali and Ahmadi, 2003; Tangestani, 2003; Ercanoğlu and Gökceoğlu, 2004; Duman et al., 2005; Komac and Ribičič, 2006].

In light of this lack of consensus, the maximum ranges fixed for the contact of the e-atlas has been based on the resolution chosen for the final output layers (1 km) as follows:

- 5000 metres for roads and drainage networks
- 10 000 metres for geological faults.

As an example, the following formula is used for reclassifying the distance to a road or hydrographical network assigning the value of 0 to $R_{\max}$ and 4 to $R_{\min}$:

$$x_i = \frac{(R_i - 5000\text{ metres})}{(0\text{ metres} - 5000\text{ metres})} \times (4 - 0) \qquad \text{Equation 2}$$

with: x_i = ordinal value
R_i = raw data value.

As R_i increases (gets further from the feature) x_i decreases. Locations more than 5000 metres from a feature are considered too distant to be affected. For these locations x_i is assigned a value of 0 (an ordinal class of 0).

2.3.1.2 Reclassification of causal factors presenting a positive correlation

Precipitation, slope, and relative elevation are all positively correlated to landside susceptibility. Areas with high annual daily maximum precipitation with a return period of five years, steep slope and a large relative elevation have a high susceptibility to landslides and the converse is also true. Areas presenting the highest values are therefore assigned to an ordinal group with a value of 4 while areas with the lowest values are assigned to an ordinal group with a value of 0 using the following formula:

$$x_i = \frac{(R_i - R_{\min})}{(R_{\max} - R_{\min})} \times \text{standardized range} \qquad \text{Equation 3}$$

with: $R_{\min}$ = minimum value of the pixel found in the dataset
$R_{\max}$ = maximum value of the pixel found in the dataset
R_i = the value of a pixel having the value between $R_{\min}$ and $R_{\max}$
x_i = the ordinal value assigned to a pixel with a raw value of R_i
standardized range = 4 × (the highest value of ordinal class)

2.3.2 Reclassification of the discrete data layers

The other factors (land cover and soil texture) are qualitative (discrete) in nature. The measurements for these data are assigned to a finite number of nominal classes that are not associated with quantities (e.g. is the land cover savannah or grassland; is the soil texture fine or medium, etc.?).

The methods used in order to convert these qualitative classes into ordinal ones are presented in the following sections.

2.3.2.1 Reclassification of the landcover layer

In a first stage, the original Global Land Cover 2000 classification is aggregated into eight simplified classifications based on vegetation density. In a second stage, an ordinal value is attributed to each simplified class according to match with the positive correlation that exists between landcover and landslide susceptibility, the lower the density of the vegetation the higher landslide susceptibility [Varnes, 1978; Sidle, Pearce, and O'Loughlin, 1985]. The result of this process is reported in Table 2.

Table 2. Table used for the reclassification of the land cover layer into ordinal values

Landscan classification	Simplified classification	Ordinal value
Barren	Bare ground	5
Irrigated cropland	Dense vegetation	1
Cropland/grassland	Dense vegetation	1
Cropland/woodland	Dense vegetation	1
Savannah	Dense vegetation	1
Deciduous broadleaf forest	Dense vegetation	1
Deciduous needleleaf forest	Dense vegetation	1
Evergreen broadleaf forest	Dense vegetation	1
Evergreen needleleaf forest	Dense vegetation	1
Mixed forest	Dense vegetation	1
Herbaceous wetland	Dense vegetation	1
Wooded wetland	Dense vegetation	1
Scrubland	Fairly dense vegetation	2
Mixed tundra	Fairly dense vegetation	2
Dry cropland and pasture	Low dense vegetation	3
Grassland	Low dense vegetation	3
Scrubland/grassland	Low dense vegetation	3
Wooded tundra	Low dense vegetation	3
Herbaceous tundra	Low dense vegetation	3
Snow or ice	Snow or ice	4
Unclassified	Unclassified	3
Developed	Urban and built-up area	3
Partly developed	Urban and built-up area	2
Water	Water	5

2.3.2.2 Soil texture

As with land cover, soil texture categories are reclassified into ordinal classes based on their hydraulic properties and susceptibility to landslides and mass-wasting events [Zobler, 1986]. Table 3 presents the result of this process.

Table 3. Table used for the reclassification of the soil texture layer into ordinal values

Soil texture	Ordinal value
Coarse	2
Medium	3
Fine	4
Unsuitable	1

2.4 Prioritization (weighting) of the causal factors

The causal factors used in this analysis exert varying degrees of influence on the overall likelihood for a landslide to occur in a given area. To account for these differences in significance, a weight should be give to each causal factor so that statistically the more influential factors exert an appropriate amount of influence on the calculation.

There is a wide variety of techniques used for weighting factors in a multi-criteria analysis [Simos, 1990]. The weighting method used in this analysis is pairwise comparison because it allows for the development and prioritization of factor weights based upon quantitative input from numerous experts.

Pairwise comparison was developed in the context of the analytical hierarchy process (AHP) by Thomas Saaty [Saaty, 1977]. The AHP model is a nonlinear method of group problem-solving and was designed to accommodate human judgement in a logical way depending on imagination, experience and knowledge of the problem [Saaty, 1990]. This method employs the use of verbal comparisons such as “more important” or “strongly more important”; which enables the AHP to create a matrix of weights that correspond with the decision-makers’ preferences. It also provides an organized structure for group discussions and helps the decision-making group to set criteria weights.

With pairwise comparison, each factor is ranked verbally by importance and then converted into a scale going from 1 to 9. This scale is then normalized to obtain values going between 0 and 1, which correspond to the weights needed for the application of the approach.

2.4.1 Prioritization of the causal factors

Each causal factor has been verbally prioritized relative to the other ones with regard to its importance in determining landslide susceptibility using the verbal judgements reported in Table 4. These verbal judgements were then converted into ordinal values between 0 and 9 as an indication of their relative level of importance (Table 4).

Based on an individual’s responses, the corresponding ordinal values are entered into a pairwise comparison matrix (Table 5).

For example in Table 5, the number 3 entered at the intersection of the landuse row and the relative elevation column (in bold) means that landuse is considered as moderately more important than the relative elevation in determining landslide susceptibility.

If this statement is true then the inverse is also correct, which is indicated by the entry of 1/3 (also in bold) found at the intersection of the relative elevation row and the landuse column.

As a final step, the values in each column are summed and the total placed in the bottom row.

Table 4. Verbal judgments and corresponding ordinal values used for the pairwise comparison analysis

Verbal judgment	Value
Extremely more important	9
	8
Very strongly more important	7
	6
Strongly more important	5
	4
Moderately more important	3
	2
Equally important	1
	1/2
Moderately less important	1/3
	1/4
Strongly less important	1/5
	1/6
Very strongly less important	1/7
	1/8
Extremely less important	1/9

Table 5. Result of the pairwise comparison analysis conducted in the context of the present work

	Annual daily maximum precipitation 5 years)	Distance from faults	Relative elevation	Distance from roads	Distance from drainage networks	Soil texture	Land use
Annual daily maximum precipitation (5 years)	1	6	5	4	2	1/2	3
Distance from faults	1/6	1	1/2	1/3	1/5	1/7	1/4
Relative elevation	1/5	2	1	1/2	1/4	1/6	1/3
Distance from roads	1/4	3	2	1	1/3	1/5	1/2
Distance from drainage networks	1/2	4	4	3	1	1/3	2
Soil texture	2	7	6	5	3	1	4
Land use	1/3	5	3	2	1/2	1/4	1
Total	4.45	28	21.50	15.83	7.28	2.59	11.08

2.4.2 Calculation of the weights for each causal factor

Once the pairwise comparison matrixes completed, individual causal factor weights are recalculated.

This is done by firstly by converting each ordinal value in Table 5 to a percentage of the sum by column. The result of this operation on the values reported in Table 5 is presented in Table 6.

The weight for each causal factor, which in fact corresponds to the percentage of landslide susceptibility that can be attributed to this factor, is then calculated as the mean value for each of the row (black column in Table 6). As check of the integrity of the calculation, the weights obtained should all sum up to 1.

Table 6. Result of the conversion of the ordinal values reported in table 5 into percentages

	Annual daily maximum precipitation (5 years)	**Distance from faults**	**Relative elevation**	**Distance from roads**	**Distance from drainage networks**	**Soil texture**	**Land cover**	**Mean (factor weights)**
Annual daily maximum precipitation (5 years)	0.22	0.21	0.23	0.25	0.27	0.27	0.19	0.237
Distance from faults	0.04	0.04	0.02	0.02	0.03	0.02	0.06	0.032
Relative elevation	0.04	0.07	0.05	0.03	0.03	0.03	0.06	0.046
Distance from roads	0.06	0.11	0.09	0.06	0.05	0.05	0.08	0.070
Distance from drainage networks	0.11	0.14	0.19	0.19	0.14	0.18	0.13	0.154
Soil texture	0.45	0.25	0.28	0.32	0.41	0.36	0.39	0.350
Landcover	0.07	0.18	0.14	0.13	0.07	0.09	0.10	0.111
						Sum		1.00

2.5 Creation of the intensity level of landslide hazard distribution maps

After having standardized the distribution of the causal factor (except the slope) according to a continuous scale and having associated a weight with each of them, the weighted linear combination (WLC) method has been used. This method multiplies each standardized causal factor distribution map by its corresponding weight to obtain weighted pixel scores. The weighted pixel scores are then summed together to yield the intermediate landslide susceptibility distribution map. This map has been reclassifying into five classes using the linear scaling technique described in section 2.2.

Once this done, the intensity level of the final landslide hazard distribution map is derived by combining the class of the intermediate landslide susceptibility distribution map with the class of the slope map.

3. Implementation of the methodology

This chapter describes how the methodology presented in section 2 was implemented using the software listed in section 3.1.

The names of the files are reported in bold in the text. When "*" follows the file name this indicates input data that are described in the *Methodology and implementation process for generating the dataset* document that can also be found in the first volume of the e-atlas.

3.1 Required software

The implementation of the methodology and processes presented in this document requires the following software:

- ArcView 3.x with the Spatial Analyst 1.1 extension, both developed by the Environmental Systems Research Institute (ESRI) Inc., for the geospatial operations

The following publicly available scripts and extensions which are accessible directly in the e-atlas DVD (in the tools section) have also been used:

- Grid Utilities v1.1 (file: Grid01.avx)
- Grid Analyst (GridAnalyst.avx)
- XTools (Xtoolsmh.avx)
- Grid and Theme Projector v.2 (grid_theme_prj.avx)
- Grid Transformation Tool (sptrnsfrm.avx).

These scripts have to be uploaded in ArcView before applying any of the process described in the following sections.

3.2 Preparation of the causal factors

This section describes the process applied to the different input data layers to obtain the spatial distribution of the causal factors.

3.2.1 Computing of the distance from roads, faults and the drainage networks

The distance from the features of three of the causal factors (roads, drainage networks and geological faults) is derived by calculating a location's minimum distance from each of these features. This section describes the processes which have been applied.

3.2.1.1 Distance from the roads and faults

The following steps are applied in order to compute the distance from the road network and from the faults:

1. In ArcView, upload the road network **st_ar_roads.shp*** and the faults **st_ar_tectonic.shp*** shape files in a view.

2. Make **st_ar_roads.shp** the active theme and open its attribute table.

3. Use the "query builder" tool and select all the records corresponding to "Motorway/Highway", "Major Trunk Roads" and "Primary Roads".

4. Use the Theme>Convert to Shapefile function to create a shape file that contains the features selected in point 3.

5. Using the process outlined in Annex 1, project the resulting shape file from the Geographic projection into the Equal-Area Cylindrical one in order to switch the map units from decimal degrees to metres.

6. Save the result shape file as **st_ar_roads_m.shp**.

7. Use the Analysis>Find Distance function to create a grid of distances from the roads in meters using the following specifications for the Output Grid:
    a. Output Grid Extent = Same as Display
    b. Output Grid Cell Size = As Specified Below
    c. Cell Size = 1000 m
    d. use the default number of rows and columns
    e. click OK.

8. Use the following steps to clip the output of step 7 to the region covered in this version of the e-atlas's international boundaries:
    a. make sure that the Grid Analyst extension is uploaded in ArcView
    b. upload the international boundary level used for the e-atlas **st_ar_int_bord.shp***
    c. make the projected grid created in step 7 the active theme and use the Grid Analyst>Extract Grid Theme Using Polygon function

  d. select the **st_ar_int_bord.shp** from the drop list as the layer to be used as the reference for the clipping
  e. make the new output grid the active theme and use the Theme>Convert to Grid function saving it as **st_ar_dist_road_m**.

9. Unproject the **st_ar_dist_road_m** grid from the Equal-Area Cylindrical projection into the Geographic one using the process outlined in Annex 2 and save the result as **st_ar_dist_roads**.

10. Repeat steps 2 to 9 on the faults distribution layer **st_ar_tectonic.shp*** keeping all the features when measuring the distance and saving the resulting grid under **st_ar_dist_faults**.

3.2.1.2 Distance from the drainage network

The following steps are applied in order to compute the distance from the drainage network.

1. Use the process outlined in section 3.2.1.1 to generate two distance grids, one for the line part (**st_ar_drain_l.shp***) and one for the polygon part (**st_ar_drain_p.shp***) of the drainage dataset. Name the resulting outputs respectively **st_ar_dist_drain_l** and **st_ar_dist_drain_p**. This has to be done separately as ArcView cannot treat lines and polygons at the same time.

2. Derive the minimum distance from the drainage network when aggregating both the **st_ar_dist_drain_l** and **st_ar_dist_drain_p** output grids together using the following process:
   a. use the Analysis>Map Calculator function and type the following formula in the calculation window: ([st_ar_dist_drain_l]–[st_ar_dist_drain_p]). The resulting grid is automatically saved under **Map calculation 1**
   b. use the Analysis>Reclassify function and reclassify the negative value in **Map calculation 1** as 1 and all of the rest as NoData. By default the resulting grid is named **Reclass of Map calculation 1**
   c. use the Analysis>Map Calculator function and type the following formula in the calculation window: ([Reclass of Map calculation 1]*[st_ar_dist_drain_l]). The resulting grid is named **Map calculation 2**
   d. use the Analysis>Map Calculator function and type the following formula in the calculation window: ([st_ar_dist_drain_p]–[st_ar_dist_drain_l]). The resulting grid is named **Map calculation 3**
   e. use the Analysis>Reclassify function and reclassify the negative values for **Map calculation 3** as 1 and all of the rest as NoData. By default the resulting grid is named **Reclass of Map calculation 3**
   f. use the Analysis>Map Calculator function and type the following formula in the calculation window: ([Reclass of Map calculation 3]*[st_ar_dist_drain_p]). The resulting grid is named **Map calculation 4**
   g. use the Transform Grid>Merge function to merge **Map calculation 2** and **Map calculation 4** together and create a grid where each cell corresponds to the minimum distance from the drainage network (lines or polygons)
   h. use the Theme>Save Data Set function to save the final grid as **st_ar_dist_drain**.

3.2.2 Creation of the relative elevation distribution layer

In a grid, the relative elevation corresponds to the difference in elevation that exists between a cell and the lowest adjacent eight cells. The process used in order to compute this layer in the context of the atlas is presented here:

1. In ArcView, upload the Digital Elevation Model (DEM) layer for the region covered in this version of the e-atlas **st_ar_dem*** in a view.

2. Make the **st_ar_dem** grid the active theme.

3. Use the Analysis>Neighborhood Statistics function and specify the following in the Neighborhood Statistics window:
    a. Statistic = Minimum
    b. the type of neighbourhood analysis under Neighborhood = Rectangle
    c. in the cell dial, Width =3 and Height = 3
    d. the resulting grid is named as **NbrMin of st_ar_dem**.

4. Use the Analysis>Map Calculator function and type the following formula in the calculator window: ([st_ar_dem]–[NbrMin of st_ar_dem]).

5. Save the resulting grid as **st_ar_rel_elev**.

3.3 Reclassification of the causal factor distribution layers

The distribution layers for the different causal factors being ready, the next step is to reclassifying these layers according to an ordinal scale from 0 to 4. This process is described in the following sections.

3.3.1 Reclassification for the distance from roads, drainage networks

The distance from roads and the drainage network are negatively correlated with landslide susceptibility (see section 2.2.1). In addition to that it was decided that roads or rivers located further away than 5000 metres would not have any effect on landslide susceptibility (see section 2.2.1.1).

This steps presented here describe how the distance from roads and the drainage network distribution layers were reclassified in order to obtain values decreasing from 4, when the distance is equal to 0, to 0 when the distance is 5000 metres.

1. In ArcView, upload the distance from the roads **st_ar_dist_roads** and from the drainage network **st_ar_dist_drain** distribution grids.

2. Use the Analysis>Map Calculator function and enter the following formula in the calculator window: (([st_ar_dist_roads]–5000)*(–0.0008)). The resulting grid is automatically named **Map calculation 1**.

3. Use the Analysis>Map Query function and select all the cells part of **Map calculation 1** that present a value > 0. The output grid, which is automatically named **Map Query 1**,

assigns a value of 1 to cells presenting a value below 5000 metres and a value of 0 to cells presenting a value above 5000 metres.

4. Use the Analysis>Map Calculator function and enter the following formula in the calculator window: ([Map calculation 1]*[Map Query 1]). Name the resulting grid **st_ar_roads_scr**. This grid shows the distance from roads scores on a 0–4 scale.

5. Repeat steps 2 to 4 on the distance from the drainage network distribution grid (**st_ar_dist_drain**) and save the result as **st_ar_drn_scr**.

3.3.2 Reclassification for the distance from faults

Similar to the distance from roads and drainage networks, the distance from faults is negatively correlated to landslide susceptibility, but has a distance of effect of 10 000 metres.

The process used to rescale this grid is therefore identical to the process described for the roads and drainage networks in section 3.3.1 except that the formula to be used in step 2 should be the following one: (([st_ar_dist_ faults]–10000)*(–0.0004)). The resulting grid should be saved as **st_ar_faults_scr**.

3.3.3 Reclassification for the precipitations and relative elevation

The annual daily maximum precipitation and relative elevation rasters are positively correlated to landslide susceptibility. This means that the areas with the highest measurements are assigned a value of 4, and those with the lowest measurements a value of 0.

The process used to reclassify these grids into a scale between 0 and 4 is outlined below:

1. In ArcView, upload the five year return period maximum daily precipitation **st_ar_prec_5*** and relative elevation **st_ar_rel_elev** in a view.

2. Make **st_ar_prec_5*** the active theme.

3. Use the Theme>Edit Legend function and select Statistics in the Legend Editor window. Note the minimum and maximum value appearing in the grid.

4. Use the Analysis>Map Calculator function and enter the following formula in the calculator window: (([st_ar_prec_5]–Rmin)*4)/(Rmax–Rmin)
   with: Rmin = minimum value found in the grid at point 3
   Rmax= maximum value found in the grid at point 3.
   Standardized range = 4.

5. Save the resulting grid as **st_ar_prec_5_scr**.

6. Repeat steps 2 to 5 on the relative elevation layer, saving the resulting grid as **st_ar_rel_elev_scr**.

3.3.4 Reclassification for the slope layer

The following process is used to reclassify the slope distribution map according to the selected scale.

1. Make **st_ar_slp_p*** the active theme.

2. Use the Analysis>Reclassify module to reclassify this grid according to the classification scheme reported in Table 1.

3. Name the output grid **st_ar_slp_scr**.

3.3.5 Reclassification for the landcover layer

The following process is used to reclassify the landcover distribution map according to the selected scale.

1. In ArcView, upload the Landcover distribution grid **st_ar_lc*** and make it the active theme.

2. Use the Analysis>Reclassify function to reclassify the grid according to the classification reported in Table 2.

3. Save the output grid as **st_ar_lc_scr**.

3.3.6 Reclassification for the soil texture layer

The following process is used to reclassify the soil texture distribution map according to the selected scale.

1. Make **st_ar_soil_text*** the active theme.

2. Use the Analysis/Reclassify module to reclassify this grid according to the classification scheme reported in Table 3.

3. Name the output grid **st_ar_soil_txt_scr**.

3.4 Creation of the intensity level of landslide hazard distribution map

The reclassified causal factor distribution layers (except slope) are combined with the weights resulting from the pairwise comparison analysis (Table 8) using the weighted linear combination (WLC) method as follows.

1. In ArcView, upload all the reclassified causal factor distribution layers **st_ar_soil_txt_scr**, **st_ar_prec_scr**, **st_ar_faults_scr**, **st_ar_rel_elev_scr**, **st_ar_drn_scr**, **st_ar_roads_scr** and **st_ar_lc_scr**.

2. Use the Analysis/Map Calculator function and enter the following formula in the calculator window: ([st_ar_soil_txt_scr]*0.350)+(st_ar_prec_scr]*0.237)+ ([st_ar_faults_scr]*0.032)+([st_ar_rel_elev_scr]*0.046)+([st_ar_drn_scr]*0.154)+ ([st_ar_roads_scr]*0.070)+([st_ar_lc_scr]*0.111).

3. Save the output grid as **st_ar_fct_nslp**.

4. Reclassify the **st_ar_fct_nslp** into 5 classes as follows:

   Use the Analysis>Reclassify function and specify the following in the Reclassify Value window that appears:

   - click on the Classification Field and ensure it reads Values
   - click the Classify button, and change the setting to read Equal Interval for Type and 5 for the Number of Classes; click OK

   - save the resulting as **st_ar_fct_cl**.

5. Derive the intensity level of the landslide hazard distribution map by combining the class of **st_ar_fct_cl** with the class of the slope map **st_ar_slp_scr** using the following process:

   a. make sure that the Grid Transformation Tool extension is uploaded in ArcView.
   b. use the Transform Grid>Combine function to combine the **st_ar_fct_cl** and **st_ar_slp_scr**
   c. name the output grid **combin_y**. The resulting grid will contains the values of the susceptibility classes for each grid in separated columns **st_ar_fct_cl** and **st_ar_slp_scr**
   d. make the **combin_y** the active grid and open its attribute table
   e. add a field called “landslide” in this attribute table
   f. select the header of the “landslide” column and enter the values according to the table 7

Table 7. Matrix used for the generating the intensity level of the landslide hazard distribution map

Landslide factors	Slope	Landslide
1	1	1
2	1	1
3	1	1
4	1	2
5	1	2
1	2	1
2	2	2
3	2	2
4	2	3
5	2	3
1	3	3
2	3	3
3	3	4
4	3	4
5	3	5
1	4	3
2	4	4
3	4	5
4	4	5
5	4	5

g. use the Analysis>Map Calculator function and type the following formula in the window: [combin_landslide] to create a grid where each cell contains the intensity level of the landslide hazard distribution map
h. save the resulting grid as **st_ar_lds_cl**.

6. In order to reduce the large amounts of neighbourhood variation, go to the Generalize Grid menu and apply the Majority Filter function on **st_ar_lds_cl**.

7. Save the output grid as **st_ar_lds_cl_cln**.

The map resulting from the application of this approach for the European Region is reported in Figure 4. Please refer to the e-atlas DVD itself for the maps covering the other two WHO Regions. The associated metadata for these layers can be found in Annex 3.

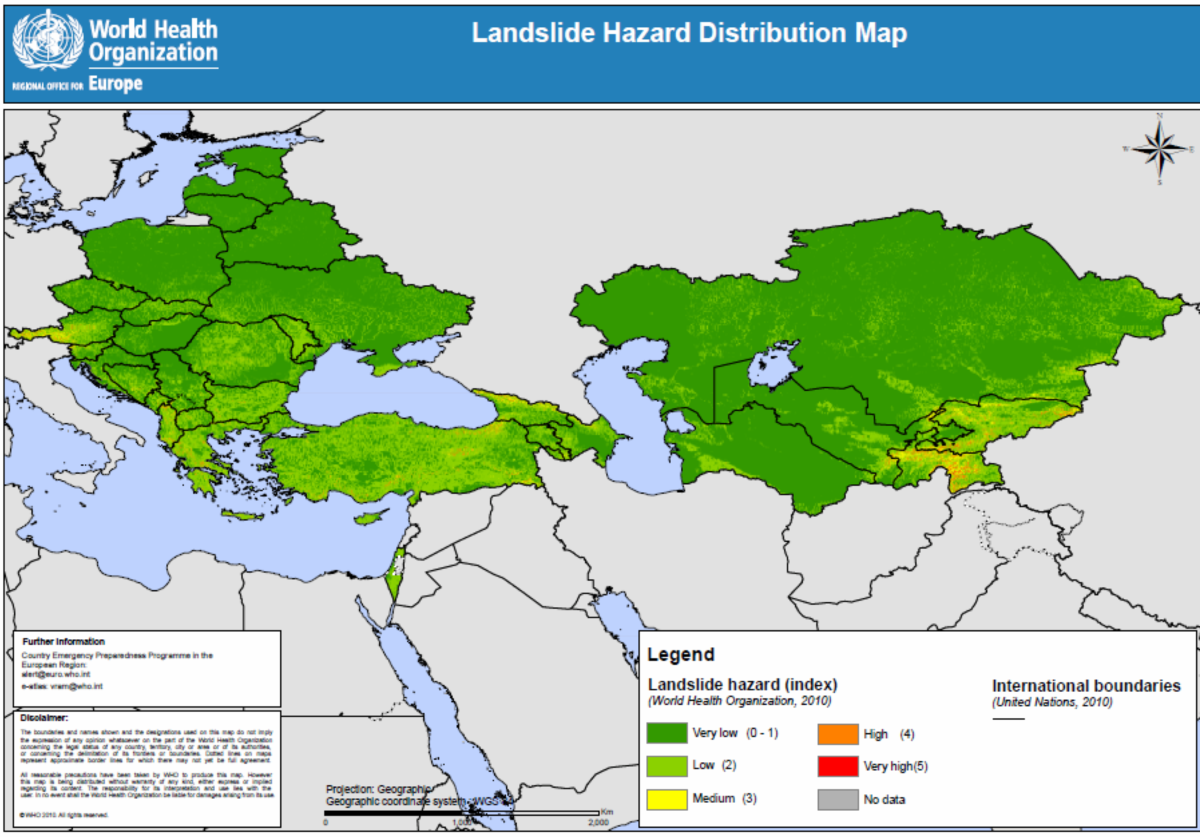

Figure 4. Landslide hazard distribution map for the countries of the European Region covered in this version of the *WHO e-atlas of disaster risk*

References and further reading

Anbalagan R, 1992. Landslide hazard evaluation and zonation mapping in mountainous terrain. *Engineering geology*, 32:269–77.

Anbalagan R, Singh B, 1996. Landslide hazard and risk assessment mapping of mountainous terrains—a case study from Kumaun Himalaya, India. *Engineering geology*, 43:237–46.

Atkinson PM, Massari R, 1998. Generalised linear modelling of susceptibility to landsliding in the Central Appenines, Italy. *Computers & geosciences*, 24(4):373–85.

Ayalew L, Yamagishi H, 2004. The application of GIS-based logistic regression for landslide susceptibility mapping in the Kakuda-Yahiko Mountains, Central Japan, *Geomorphology*, 65(1–2):15–31.

Ayenew T, Barbieri G, 2005. Inventory of landslides and susceptibility mapping in the Dessie area, northern Ethiopia. *Engineering geology*, 77(1–2):1–15.

Barisone G, Bottino G, 1990. A practical approach for hazard evaluation of rock slopes in mountainous areas. *Proceedings of the 6th IAEG Congress*:1509–15. Rotterdam, Balkema.

Barredo JI, Benavides A, Hervás J, van Westen CJ, 2000. Comparing heuristic landslide hazard assessment techniques using GIS in the Tirajana basin, Gran Canaria Island, Spain, *International journal of applied earth observation and geoinformation*, 2(1):9–23.

Baum RL, Chleborad AF, Schuster RL, 1998. Landslides triggered by the winter 1996–97 storms in the Puget Lowland, Washington. Reston, Virginia, US Geological Survey, Open-File Report 98-239. At http://pubs.er.usgs.gov/usgspubs/ofr/ofr98239 [Accessed December 15, 2010]

Bender S, 1991. *Primer on natural hazard management in integrated regional development planning*. Washington DC, Department of Regional Development and Environment, Executive Secretariat for Economic and Social Affairs, Organization of American States.

Brabb EE, 1984. Innovative approaches to landslide hazard mapping. *Proceedings of the 4th International Symposium on Landslides*, vol 1:307–24. Toronto, Canadian Geotechnical Society.

Carrara A, 1989. Landslide hazard mapping by statistical methods: a "black-box" model approach. *Proceedings of the International Workshop on Natural Disasters in European–Mediterranean Countries. Perugia, June 27–July 1, 1988*:205–24. Rome, Consiglio Nazionale delle Ricerche/US National Science Foundation.

Carrara A, Cardinali M, Detti R, Guzzetti F, Pasqui V, Reichenbach P, 1991. GIS techniques and statistical models in evaluating landslide hazard. *Earth surface processes and landforms*, 16(5):427–45.

Clerici A, Perego S, Tellini C, Vescovi P, 2002. A procedure for landslide susceptibility zonation by the conditional analysis method. *Geomorphology*, 48:349–64.

Dai FC, Lee CF, 2002. Landslide characteristics and slope instability modeling using GIS, Lantau Island, Hong Kong. *Geomorphology*, 42:213–28.

Donati L, Turrini MC, 2002. An objective method to rank the importance of the factors predisposing to landslides with the GIS methodology: application to an area of the Apennines (Valnerina; Perugia, Italy). *Engineering geology*, 63:277–89.

Duman TY, Can T, Gökçeoğlu C, Nefeslioğlu HA, 2005. Landslide susceptibility mapping of Çekmece area (Istanbul, Turkey) by conditional probability. *Hydrology and earth system sciences discussions*, 2:155–208.

Eastman JR, 2003. *Idrisi Kilimanjaro: guide to GIS and image processing version 14.00.* Worcester, Massachusetts, Clark University.

Ercanoğlu M, Gökçeoğlu C, 2002. Assessment of landslide susceptibility for a landslide-prone area (north of Yenice, NW Turkey) by fuzzy approach, *Environmental geology*, 41(6):720–30.

Ercanoğlu M, Gökçeoğlu C, Van Asch ThWJ, 2004. Landslide susceptibility zoning north of Yenice (NW Turkey) by multivariate statistical techniques. *Natural hazards*, 32:1–23.

Ercanoğlu M, Gökçeoğlu C, 2004. Use of fuzzy relations to produce landslide susceptibility map of a landslide prone area (West Black Sea Region, Turkey), *Engineering geology*, 75:229–50.

Esmali A, Ahmadi H, 2003. Using GIS & RS in mass movements hazard zonation—a case study in Germichay Watershed, Ardebil, Iran. Map India Conference 2003. At http://www.gisdevelopment.net/application/natural_hazards/landslides/ma03004.htm [Accessed December 15, 2010]

Glassey PJ, Forsyth PJ, Turnbull M, 1997. A GIS-based hazard information system: Dunedin pilot project. *IPENZ transactions (general)*, 24(1). At http://www.ipenz.org.nz/ipenz/publications/transactions/Transactions97/general/4glassey.pdf [Accessed December 15, 2010]

Gökçeoğlu C, Aksoy H, 1996. Landslide susceptibility mapping of the slopes in the residual soils of the Mengen region (Turkey) by deterministic stability analyses and image processing techniques. *Engineering geology*, 44:147–61.

Gomes A, Gaspar JL, Goulart C, Queiroz G, 2005. Evaluation of landslide susceptibility of Sete Cidades Volcano (S. Miguel Island, Azores). *Natural hazards and earth system sciences*, 5:251–57.

Gupta RP, Joshi BC, 1990. Landslide hazard zoning using the GIS approach—a case study from the Ramganga Catchment, Himalayas. *Engineering geology*, 28:119–31.

Guzzetti F, Carrara A, Cardinali M, Reichenbach P, 1999. Landslide hazard evaluation: a review of current techniques and their application in a multi-scale study, central Italy, *Geomorphology*, 31:181–216.

Guzzetti F, Cardinali M, Reichenbach P, Carrara A, 2000. Comparing landslide maps: a case study in the upper Tiber river basin, central Italy. *Environmental management*, 25(3):247–63.

Hansen A, 1984. Landslide hazard analysis. In: Brunsden D, Prior DB, eds., *Slope instability*. New York, Wiley, 523–602

Hansen A, Franks CAM, 1991. Characterization and mapping of earthquake triggered landslides for seismic zonation. *Proceedings of the 4th International Conference on Seismic Zonation, Stanford, California, August 26–29, 1991*:149–95.

Jager S, Wieczorek GF, 1994. Landslide susceptibility in the Tully Valley area, Finger Lakes region. Washington. Reston, Virginia, US Geological Survey, Open-File Report 94-615. At http://pubs.er.usgs.gov/usgspubs/ofr/ofr94615 [Accessed December 15, 2010]

Jakob M, 2000. The impacts of logging on landslide activity at Clayoquot Sound, British Columbia. *Catena*, 38:279–300.

Kelarestaghi A, 2003. Investigation of effective factors on landslides occurrence and landslide hazard zonation—case study Shirin Rood drainage basin, Sari, Iran. At http://www.gisdevelopment.net/application/natural_hazards/landslides/ma03003pf.htm [Accessed December 15, 2010]

Komac M, Ribičič M, 2006. Landslide susceptibility map of Slovenia at scale 1:250.000, *Geophysical research abstracts*, 8:03990. At http://www.cosis.net/abstracts/EGU06/03990/EGU06-J-03990.pdf [Accessed December 15, 2010]

Koukis G, Ziourkas C, 1991. Slope instability phenomena in Greece: a statistical analysis. *Bulletin of the International Association of Engineering Geologists*, 43:47–60.

Luzi L, Pergalani F, 1999. Slope instability in static and dynamic conditions for urban planning: the “Oltre Po Pavese” case history (Regione Lombardia—Italy). *Natural hazards*, 20(1):57–82.

Maharaj R, 1993. Landslide processes and landslide susceptibility analysis from an upland watershed: a case study from St Andrew, Jamaica, West Indies, *Engineering geology*, 34(1–2):53–79.

Martinez A, 2003. *Elaboration d’un SIG pour la gestion des zones à risque de glissements de terrain dans le quartier de Villatina Medellín, Colombie*. Certificate of Geomatics, University of Geneva [in French].

Nagarajan R, Roy A, Vinod Kumar R, Mukherjee A, Khire MV, 2000. Landslide hazard susceptibility mapping based on terrain and climatic factors for tropical monsoon regions. *Bulletin of engineering geology and the environment*, 58:275–87.

Pachauri AK and Pant M, 1992. Landslide hazard mapping based on geological attributes, *Engineering geology*, 32:81–100.

Pachauri AK, Gupta PV and Chander R, 1998. Landslide zoning in a part of the Garhwal Himalayas. *Environmental geology*, 36(3–4):325–34.

Ramakrishnan SS, Kumar VS, Sadiq Z, Venugopal K, 2002. Landslide zonation for hill area development. At http://www.gisdevelopment.net/application/natural_hazards/landslides/nhls0013pf.htm [Accessed December 15, 2010]

Roth RA, 1983. Factors affecting landslide susceptibility in San Mateo County, California, *Bulletin of the Association of Engineering Geologists*, 20(4):353–72.

Saaty TL, 1977. A scaling method for priorities in hierarchical structures. *Journal of mathematical psychology*, 15:234–81.

Saaty TL, 1990, Decision making for leaders: the analytical hierarch process for decision in a complex world. *Pittsburgh, Pennsylvania, RWS Publications*.

Sarkar S, Kanungo DP, 2002. Landslides in relation to terrain parameters—a remote sensing and GIS approach. At http://www.gisdevelopment.net/application/natural_hazards/landslides/nhls0010pf.htm [Accessed December 15, 2010]

Sidle RC, Pearce AJ, O'Loughlin CL, 1985. Hillslope stability and land use. Water Washington DC, American Geophysical Union. *Resources Monograph Series No. 11*.

Simos J, 1990. Evaluer l'impact sur l'environnement : une approche originale par l'analyse multicritère et la négociation. Lausanne, Swizerland, *Presses polytechniques et universitaires romandes* [in French].

Sinha LK, Paul RS, Mehta SD, 1999. Landslide hazard zonation in a part of Giri Basin, Sirmur district (H.P.) using remote sensing techniques & GIS. At http://www.gisdevelopment.net/application/natural_hazards/landslides/nhls0012pf.htm [Accessed December 15, 2010]

Suzen ML, Doyuran V, 2004. A comparison of the GIS based landslide susceptibility assessment methods: multivariate versus bivariate. *Environmental geology*, 45:665–79.

Talib JA, 1997. Slope instability and hazard zonation mapping using remote sensing and GIS Techniques in the area of Cameron Highlands, Malaysia. At http://www.gisdevelopment.net/aars/acrs/1997/ts3/ts3001pf.htm [Accessed December 15, 2010]

Tangestani MH, 2003. Landslide susceptibility mapping using the fuzzy gamma operation in a GIS, Kakan catchment area, Iran. At http://www.gisdevelopment.net/application/natural_hazards/landslides/pdf/40.pdf [Accessed December 15, 2010]

Turrini MC, Visintainer P, 1998. Proposal of a method to define areas of landslide hazard and application to an area of the Dolomites, Italy. *Engineering geology*, 50:255–65.

Van Westen CJ, Seijmonsbergen AC, Mantovani F, 1999. Comparing landslide hazard maps. *Natural hazards*, 20:137–58.

Van Westen CJ, 2003. Statistical landslide hazard analysis. At http://www.itc.nl/ilwis/applications/application05.asp [Accessed December 15, 2010]

Varnes DJ, 1978. Slope movement types and processes. In Schuster RL, Krizek RJ, eds. *Landslides, analysis, and control*, Washington DC, Transportation Research Board. Special Report 176.

Voogd H, 1983. *Multicriteria evaluations for urban and regional planning*. London, Pion Press.

Wachal DJ, Hudak PF, 2000. Mapping landslide susceptibility in Travis County, Texas, USA. *Geojournal*, 51:245–53.

Zezere JL, Ferreira AB, Rodrigues ML, 1999. Landslides in the north of Lisbon region (Portugal): conditioning and triggering factors. *Physics and chemistry of the Earth, part A: solid Earth and geodesy*, 24(10):925–34.

Zobler L, 1986. *A world soil file for global climate modeling*. New York, NASA Goddard Institute for Space Studies. NASA Technical Memorandum 87802.

Annex 1. Process followed in order to project a layer from the Geographic to the Equal-Area Cylindrical projection

In ArcView

1. Make sure that the Grid and Theme Projector v.2 extensions are uploaded.

2. Click either on the button or use the Grid Projector>Grid>Theme Projector function.

3. Select the layer to be projected from the list as the theme to project.

   In the Theme Projector window:

   a. specify the following parameters for the current projection:
      - Category = projection of the world
      - Type = Geographic
      - Current Projection Units = decimal degrees

   b. specify the following parameters for the new projection:
      - Category = projection of the world
      - Type = Equal-Area Cylindrical
      - New Projection Units = meters.

4. Save the output theme under a new name.

Annex 2. Process for projecting a layer from the Equal-Area Cylindrical to the Geographic projection

In ArcView

1. Make sure that the Grid and Theme Projector v.2 extensions are uploaded.

2. Click on the button or use the Grid Projector>Grid>Theme Projector function.

3. Select the layer to be projected from the list as the theme to project.

   In the Theme Projector window:

   a. specify the following parameters for the current projection:
      - Category = projection of the world
      - Type = Equal-Area Cylindrical
      - New Projection Units = meters

   b. specify the following parameters for the new projection:
      - Category = projection of the world
      - Type = Geographic
      - Current Projection Units = decimal degrees.

4. Save the output theme under a new name.

Annex 3. Metadata for the intensity level of landslide hazard distribution layer

Dataset title	Spatial distribution of the intensity level of landslide hazard for the WHO Regions (Africa, Eastern Mediterranean and part of Europe)
Theme keywords	WHO, Africa, Eastern Mediterranean, Europe, natural disaster, Geographic Information System (GIS), landslide, slope stability, mass-wasting
Dataset topic category	Landslide
Geographic location	The layer covers a total of 100 countries (22 for the Eastern Mediterranean, 46 for Africa and 32 for Europe)
Publication date	20110301
Data exchange format	ArcView grid
Filename	st_ar_lds_cl
Dataset edition	Second edition
Abstract	This layer contains the spatial distribution of the intensity level of landslide hazard for the WHO Regions (Africa, Eastern Mediterranean and part of Europe)
Lineage	The process used to create the intensity level of landslide hazard distribution map is described in the *Methodology and implementation process for modelling the spatial distribution of landslide hazard* document that can be found in the first volume (2nd edition) of the *WHO e-atlas of disaster risk for the WHO Regions (Africa, Eastern Mediterranean and part of Europe)*

Data quality comments	Please refer to the data specific metadata for more information regarding the quality of the grids used as input for the creation of the landslide hazard grid Because of the methods and resolution used (1 km) special care should be taken when using this dataset for application below the national level The method did not integrate lithology as this layer was not available for the WHO Regions (Africa, Eastern Mediterranean and part of Europe)
Distributor	WHO Mediterranean Centre for Health Risk Reduction (WMC)
Spatial representation type	grid
Map projection	Unprojected (Geographic)
Reference system	WGS 84 datum
Geographic box	X min: –25.358747°, X max: 91.8287° Y min: –46.978931°, Y max: 63.459827°
Resolution	30 arc-seconds (0.008333°)
Redistributions constraints	The intensity level of landslide hazard distribution layer is copyrighted. The owner of the data agrees to the use, reproduction, distribution, display, publication and dissemination at no cost to third parties of the intensity level of landslide hazard distribution layer, in any manner and in any form whatsoever, subject to the copyright and acknowledgement mentioned in these metadata
Access and use constraints	This layer may not be reproduced, changed, adapted, translated, stored in a retrieval system or transmitted in any form or by any means without prior permission of the copyright holder, except to make a security backup. Requests for permission, with a statement of purpose and extent, should be address to the VRAM programme at the WHO Mediterranean Centre for Health Risk Reduction (VRAM@who.int)
Acknowledgement	*WHO e-atlas of disaster risk for the WHO Regions (Africa, Eastern Mediterranean and part of Europe)* 2nd edition. Copyright © WHO 2011. All rights reserved

Disclaimer	All reasonable precautions have been taken by WHO to produce this layer. However this layer is being distributed without warranty of any kind, either express or implied regarding its content. The responsibility for its interpretation and use lies with the user. In no event shall the World Health Organization be liable for damages arising from its use
Online linkage	Under construction
Dataset language	English
Dataset character set	ASCII
Metadata provider	WHO Mediterranean Centre for Health Risk Reduction (WMC)
Metadata contact	El Morjani Zine El Abidine BP 3566 Poste Talborjt 80000 Agadir Morocco Telephone: +212 528 28 55 30 email: elmorjaniz@gmail.com
Metadata date	20110301
Metadata language	English
Metadata character set	ASCII
Metadata standard	ISO 19115